Journal of Optoelectronics and Advanced Materials Vol. 5, No. 2, June 2003, p. 369 - 388

REVIEW PAPER

DEFECT STRUCTURE AND LUMINESCENCE PROPERTIES OF CdTe BASED COMPOUNDS

P. Fernández*

Depto. Física de Materiales, Fac. Físicas, Univ. Complutense, 28040 Madrid, Spain

This paper reviews the most prominent features of the defect related cathodoluminescence emissions in CdTe based compounds. Two main problems are dealt with, the influence of dopants and the effect of mechanical damage. Several defect related bands have been observed between 1.4 and 0.78 eV which seem to be strongly influenced by doping and, as deduced from annealing experiments, by migration of defects. Dislocations and Cottrell atmospheres around them seem also to play an important role in the luminescence properties of these materials. Although this review is focused onto the cathodoluminescence measurements, comparison with the results obtained by other techniques (Deep Level Transient Spectroscopy, Photo Induced Current Transient Spectroscopy, Raman Spectroscopy) are referred.

(Received March 3, 2003; accepted May 8, 2003)

Keywords: CdTe, Luminescence, Defects

1. Introduction

CdTe is a wide band gap II-VI compound with promising applications as X- and γ-ray detector [1,2] and for high efficiency solar cells [3,4]. Also currently, is being successfully employed as a substrate for HgTe based epitaxial layers to be used in infrared technology [5,6]. More recently an additional interest has been stimulated by the discovery of infrared photorefractivity [7,8]. Different properties are required for the different applications, for instance infrared applications require a high room temperature resistivity ($\rho > 10^8$ Ωcm) and good photoconductivity on infrared radiation [7,8]. There exist few possibilities to get the CdTe crystals with the desirable properties by doping. These possibilities base themselves on the fact that in the undoped CdTe the main residual point defects are shallow acceptors such as the background impurities of the group I (Li, N, Cu, Ag) and their complexes with the native defects, mainly the vacancies of cadmium (V_{Cd}) [1]. For example, the high resistivity CdTe could be obtained by the compensative doping with chlorine or gallium which are the shallow donors in Te- or Cd-sublattices respectively [9, 10]. However, the doping with the impurities of V or IV groups, e.g. vanadium or germanium, can also provide the semiinsulating CdTe crystals by compensating deep donor levels [7,11].

The defect structure of CdTe substrates has been often investigated with luminescence techniques. In particular, a luminescence band normally referred as the 1.40 eV band, has been associated with recombination processes involving defects but its nature seems to be complex. Myers et al. [12] in their photoluminescence study of CdTe wafers concluded that a significant part of this band is related to surface damage, however many other authors [13-15] suggest that this emission is related to bulk defects. Photoluminescence and optical detected magnetic resonance have been used to study intrinsic defects and to relate them to luminescence bands [16,17] concluding that the A centre (cation vacancy-donor pair) is involved in the 1.4 eV band. On the other hand a luminescence band has been

* Corresponding author: arana@fis.ucm.es

reported at about 1.1-1.15 eV [17,18]. The optically detected and conventional spin resonance measurements indicate the relation of this band to Te vacancies. Since some impurities can occupy substitutional sites filling vacancies in either of the sublattices, it seems to be quite interesting to investigate the influence of different dopants on the defect structure of this material [12-20]. Also interesting is the influence of plastic deformation on deep levels. Tarbaev [19] observed plasticity of CdTe at 77 K and reported the presence of dislocation related luminescence bands near the fundamental spectral region. Babentsov et al. [20] described PL bands in the range 1.48-1.51 eV at 4 K and established that the intensity of the bands was correlated with the density of dislocation network created by mechanical treatment, however the nature of the defects involved in these emissions could not be stated. During the deformation process not only are created dislocations but also point defects involving cadmium as well as tellurium vacancies, which can have an important influence on the deep level emissions [16-19].

It was already mentioned the applicability of CdTe wafers, as well as CdTe based ternary compounds to the fabrication of different types of sensors. One of the problems encountered which restricts the use of the material is the formation of tellurium precipitates distributed randomly over the whole volume of the wafers [23-26]. The presence of these precipitates is due to peculiarities of the CdTe phase diagram, i.e. a Te rich composition in the vicinity of melting point and a strong retrograde character of solidus on Te-rich side of homogeneity region [27]. The precipitates create some technological problems related to post growth stoichiometry control. In particular, one of the main problems is the most times unpredictable transformation of the precipitates during the annealing treatments involved in ohmic contacts fabrication or during epitaxial growth [6,28-32]. It is not possible to avoid completely the presence of Te precipitates by a modification of the growth process and post-growth annealing [22,29,33,34], however some reduction in its concentration can be achieved by thermal treatments in Cd vapour [26,35,36]. In a previous work, Jayathirtha et al have carried out studies [25] on the elimination of Te precipitates by Cl doping. Nevertheless the contradictions between this work and previous studies [22,33,34] point out the necessity of further studies using different techniques.

Apart from the point defects, structural extended defects such as grain boundaries can have an important influence on the electrical properties of semiconductors, therefore many techniques have been applied to the investigation of such type of defects [37, 38]. In many cases the influence of extended defects cannot be clearly defined due to the fact that they are very effective gettering sites for point defects introduced during crystal growth or during post-growth thermal treatments. Some scanning electron microscope (SEM) techniques such as electron beam induced current (EBIC) and cathodoluminescence (CL) have a high spatial resolution which makes possible the observation of single extended defects acting as recombination centres [39].

Although the techniques used in the study of CdTe cover a wide range of beam injection methods, in this review we will concentrate on the luminescence results.

2. Experimental methods

The samples used were obtained from bulk material grown by the Bridgman method. Several dopants have been introduced to investigate their effect on the defect structure and on compensation mechanisms. More details on samples are given in Table 1. When necessary the samples were chemo-mechanically polished with a bromine methanol solution of concentration 0.1 to 5% Br_2. The concentration used depends on the amount of material we wanted to remove, i.e. on the state of the surface.

Cathodoluminescence measurements were performed in a Hitachi S-2500 Scanning Electron Microscope at temperatures between 80 and 300 K with accelerating voltage of 25 kV. The experimental set-up for spectral and panchromatic CL measurements with a North Coast EO-817 germanium detector has been previously described [37]. To record spectra, a light guide feeding the light to an Oriel 78215 computer controlled monochromator was used. In some cases to separate the contribution of the different bands in the CL images, monochromatic CL images are recorded at the fixed wavelengths corresponding to the peak positions in the CL spectra. Spectra are recorded under different focusing conditions of the electron beam on

the samples to account for the radiative centres with low concentration [15, 19, 40]. Usually by defocusing, the intensity of deep level bands increases.

3. Results and discussion

The quality of CdTe substrates has been often investigated with different characterisation techniques including photoluminescence and cathodoluminescence (CL) [12-14]. In particular, a luminescence band, normally referred as the 1.4 eV band, has been associated to recombination processes involving defects. Fig. 1 shows CL spectra at 80 K of the undoped CdTe wafer (Samples type S1 and S2). With focused electron beam only the exciton band peaked at 1.54 eV (805 nm) is observed. By defocusing, the spectrum shows the 1.40 eV (885 nm) band as well as an increase of a background emission at wavelengths longer than 1000 nm. The most intense of these bands is located at 1.1 eV. Also a band at 0.78 eV is observed. Fig. 2 shows the intensity variation of both bands along a wafer radius. Intensity of the 1.40 eV band has been measured under excitation with defocused electron beam. Fig. 3 shows a typical panchromatic CL image with bright subboundaries as well as bright spots inside the subgrains. By using optical filters, CL images corresponding to emission at wavelengths above 950 nm and 1000 nm were obtained. Images recorded with the 950 nm filter show the same luminescence space distribution than the panchromatic images, but with reduced intensity. Even with the 1000 nm filter, subboundary CL contrast is observed.

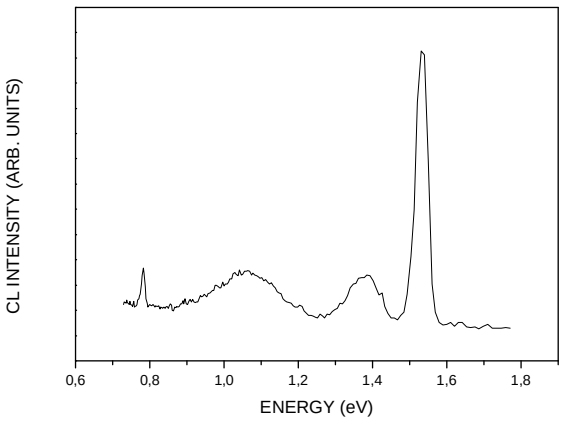

Fig. 1. CL spectra of undoped CdTe at 80 K .

Table 1. Characteristics of the samples.

S1	UNDOPED CdTe (111) JAPAN ENERGY CORPORATION $n \approx 10^{15} cm^{-3}$, ρ=28 Ω cm
S2	UNDOPED CdTe (111) GROWN BY VERTICAL BRIDGMAN METHOD
S3	Cl DOPED SAMPLES FROM JAPAN ENERGY CORPORATION $\rho = 10^{7}$ Ω cm
S4	HIGH PRESSURE BRIDGMAN METHOD, FROM AURORA TECH.CORP. UNDOPED, AND 20% Zn DOPED, $\rho=1.5\times 10^{11}$ Ω cm
S5	S1 DOPED WITH Ge IN CONCENTRATIONS $10^{17} cm^{-3}$ (Ge1 SAMPLE) AND 10^{19} cm^{-3} (Ge2 SAMPLE) , RESISTIVITIES 10^{8}-10^{9} Ω cm
S6	S1 DOPED WITH V IN CONCENTRATION $7\times 10^{19} cm^{-3}$

Further investigations on the defect structure of undoped samples have been performed by increasing the density of defects by mechanical damage. Sample from the type S1 (Table 1) were indented with a diamond indenter of an Akasi MVK-E3 microhardness system with loads from 10 g to 100 g. By this process extended as well as point defects are introduced.

Fig. 4 shows the CL image of an indentation. Quenching of luminescence in the deformed areas, in agreement with a previous work [41] is observed. For spectral CL measurements three regions were considered in addition to undeformed material: the indentation center, the rosette arms and the area between two adjacent arms. In Fig. 5a, CL spectra of the 10 g indentation are presented. The same emission bands are observed in the spectra corresponding to higher loads. Measurement of the relative intensities of the bands reveals some effect of plastic deformation besides the observed luminescence quenching. In the spectra recorded under focused electron beam the relative intensity of the 1.4 and 1.1 eV bands, compared with that of near band edge luminescence is higher in the indentations than in the undeformed material. The relative intensities of the 1.4 and 1.1 eV bands in the spectra depend on the load and on the indentation region considered. Spectral analysis of indentations also shows that both emission bands are more intense in the center than in other deformed regions with the exception of 50 g indentation in which the intensities in the rosette and in the center are comparable. It is also observed for both bands that the ratios I_{arm}/I_{center} and $I_{between}/I_{center}$ increase with applied load.

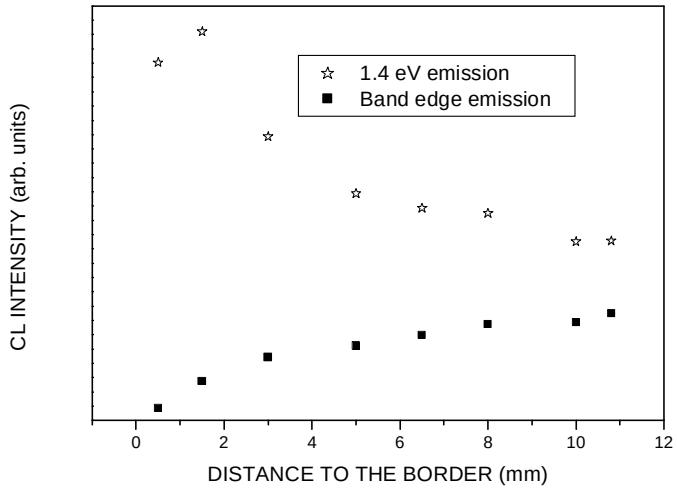

Fig. 2. Intensity distribution of exciton bands along the radius of the CdTe wafer.

Annealing causes the disappearance of the 1.4 eV band in the deformed regions while a strong emission remains in the range 0.8 to 1.1 eV. Spectra from annealed samples are shown in Fig. 5b. They are similar for deformed and undeformed regions. Topographic features of low load indentation are lost or modified during annealing due to thermal surface etching in deformed areas. This effect is relatively low in the high load indentation and correspondingly CL images could be recorded. Fig. 6 shows that annealing causes the appearance of a bright region around the indentation center.

The present observations (Fig. 4) as well as previous works [41] show that plastic deformation causes quenching of CL emission in CdTe crystals. The generation of nonradiative recombination centers during plastic deformation has been also observed in the past in other semiconductors with a spatial distribution which correlates with the dislocation distribution [42]. In addition to the general CL quenching, deformation induce relative intensity changes of emission bands. In particular, the relative intensities of the bands at 1.4 and 1.1 eV appear higher in the deformed regions. This effect has been studied by defocusing the microscope electron beam.

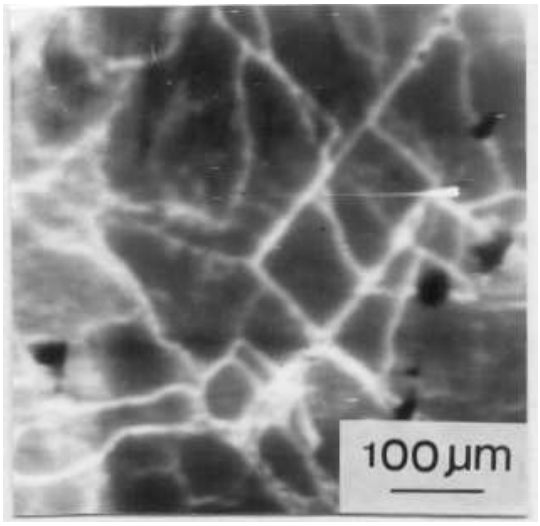

Fig. 3. Panchromatic CL image of CdTe at 80 K.

Although the total intensity in the indentation decreases as a consequence of the dislocation related non-radiative centers, radiative centers are also generated during deformation. This becomes apparent in the fact that the emission bands at 1.4 and 1.1 eV are more intense in the indentation center than in the rosette arms and have lower intensity values in the space between arms and in undeformed regions. The variation of the intensity ratio from region to region indicates that different defects are involved in these bands.

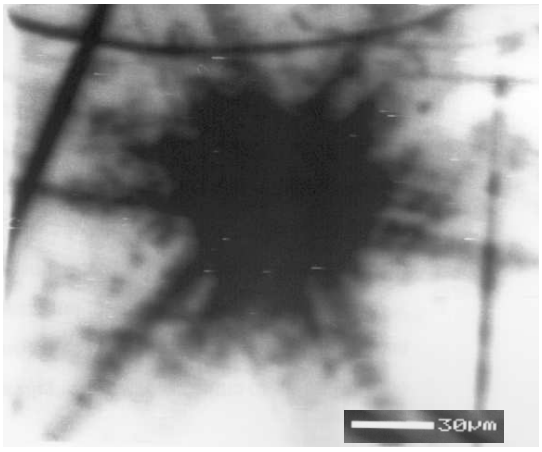

Fig. 4. Panchromatic CL image of an indentation.

As stated before, the band at 1.4 eV is related to defects involving cadmium vacancies, in particular, the A center is strongly related to this emission [16,17,19]. The relatively high intensity of this band in deformed regions could be explained by cadmium vacancy generation during the deformation and subsequent A center formation. The luminescence band peaked at 1.1 eV has been also reported [17,18]. Optically detected and conventional spin resonance measurements [17] indicate that the band is related to Te vacancies. A similar conclusion is obtained in CL experiments from annealed samples [19].

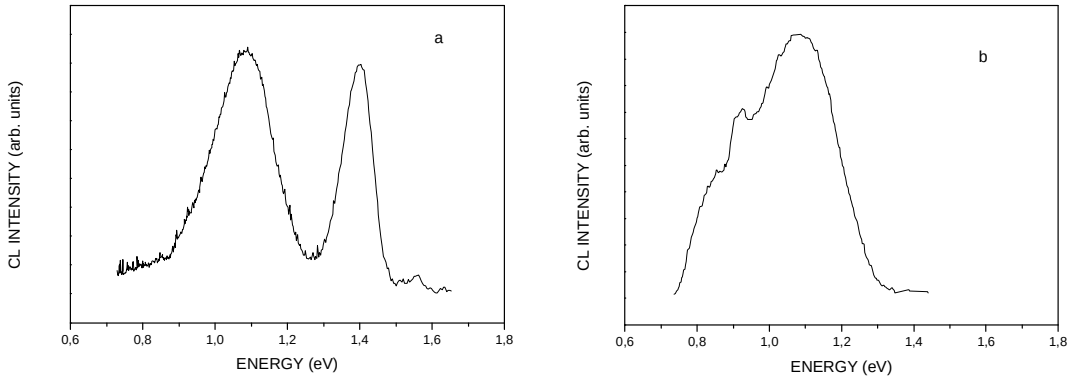

Fig. 5. CL spectra of a deformed region recorded on the rosette arm, before (a) and after (b) annealing in inert atmosphere (1h, 600 ºC).

Annealing has been previously [19] found to induce an increase of the 1.1 eV band, while the 1.4 eV band was not readily observed. This is explained by the fact that the state of the surface has a strong influence on the 1.4 eV emission [12]. The defocused spectra of the annealed samples are qualitatively similar for deformed and undeformed regions showing the 1.1, 0.9, and 0.85 eV bands. The latter two bands have been suggested [57] to be related to impurities in Cd sites.

In the spectra of annealed samples obtained with focused electron beam, near band edge emission and a broad deep level band are observed (Fig. 5b). In order to investigate the process leading to the appearance of the bright region around the indentation center during annealing, focused spectra were recorded in different regions of the indent. No increase of deep level emission was observed in the bright region but the enhanced CL emission was found to be due to higher near band emission. The formation of a bright region around an annealed indentation has been described in CL studies of CdS [43] and attributed to dislocation decoration by point defects similar to the well known process in single dislocations in some other II-VI semiconductors [44-46]. The fact that no enhancement of 1.4 or 1.1 eV bands is observed in the bright region suggests that dislocations are decorated by impurities rather than by the vacancies.

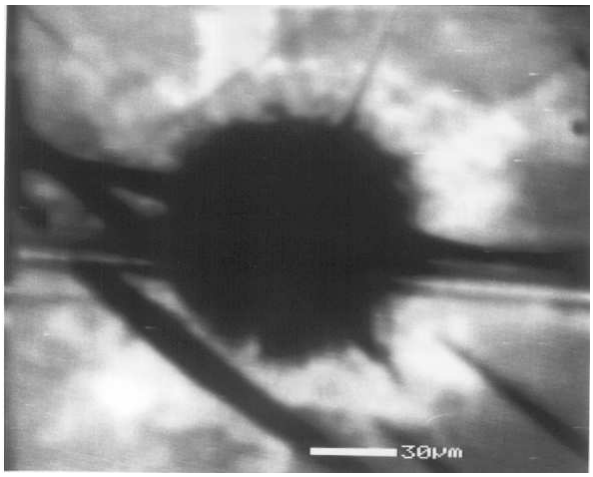

Fig. 6. Panchromatic CL image of an indentation after annealing. The dark horizontal line is a scratch caused by polishing.

As mentioned in the introduction, one of the problems of interest in technology is the presence of Te precipitates. To study the spatial distribution of Te precipitates all over the wafer volume, the wafers (type S2) were cleaved perpendicular to the [111] direction just before the CL measurements and the cleaved surface was investigated. Doing this, we have eliminated the possible influence of the wafer surface treatment [47]. An analogy between CL data obtained from the cases of Ga-melt and Cd-vapor annealings and RS measurements from the same samples was found [48].

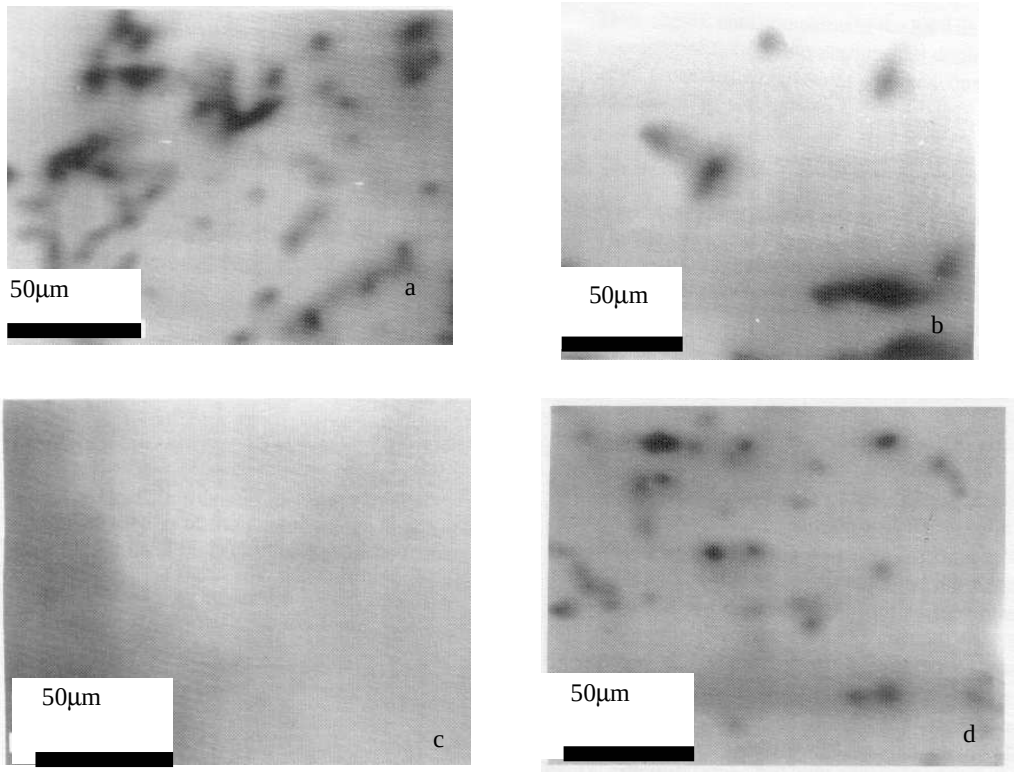

Fig. 7. Panchromatic CL images of a cross section of CdTe wafers at 80 K: (a) as-grown; (b) in the central part of cross section after annealing in Ga melt at 600 ºC for 2 h; (c) close to the wafer surface in contact with the Ga melt, after long time annealing (600 ºC, 24 h); (d) close to the opposite surface of the wafer.

Both, as-grown and annealed wafers were investigated. Samples were annealed either in liquid Ga or in Cd vapor for 2 h (short time annealing) or for 22 h (long time annealing). All the annealings were carried out in evacuated quartz ampoules at temperatures in the range 550-600 ºC. For the annealing in Cd vapor, a piece of Cd was introduced into the ampoule. For the Ga annealing, a layer or pure Ga(6N) of 0.5-1 μm thickness was deposited at room temperature (RT) on one or both sides of a wafer by spreading Ga drops. More technological details on the annealing procedures could be found elsewhere [6,29,30].

The CL images and spectra have not revealed any significant effect of doping on the transformation of Te precipitates. Fig. 7 shows typical CL images of as-grown (a) and annealed (b-d) samples. These images correspond to the regions of the wafer cross section from which CL spectra were recorded. While the as-grown wafers were of good structural quality estimated by X-ray measurements [29], their CL images exhibited a random distribution of Te precipitates over the whole volume (Fig. 7a).

After the short time annealing in Ga melt a significant improvement of the CL image contrast was usually observed in the central part of the wafer cross sections, demonstrating the disappearance of small (< 10 μm) precipitates and a reduction in the density of structural defects in the space between precipitates (Fig. 7b). On the contrary, a strong increase in the concentration of Te precipitates was seen near the surface of

the wafers which was in contact with the Ga melt. This precipitate rich region extends up to 200 μm away from the surface.

After the 24 h annealing in Ga melt a complete disappearance of Te was found to occur over the whole volume of the wafers, except in those regions near the surface. Correspondingly featureless CL images are obtained. Within a distance of about 100 μm from the wafer surface in contact with the Ga melt, the CL image shows a high density of Te precipitates, near this surface the boundary between the precipitate-free and the precipitate-rich regions is well defined (Fig. 7c). Near the opposite surface, exposed to vacuum, and due probably to gettering effect an increase in the concentration of Te precipitates is observed (Fig. 7d).

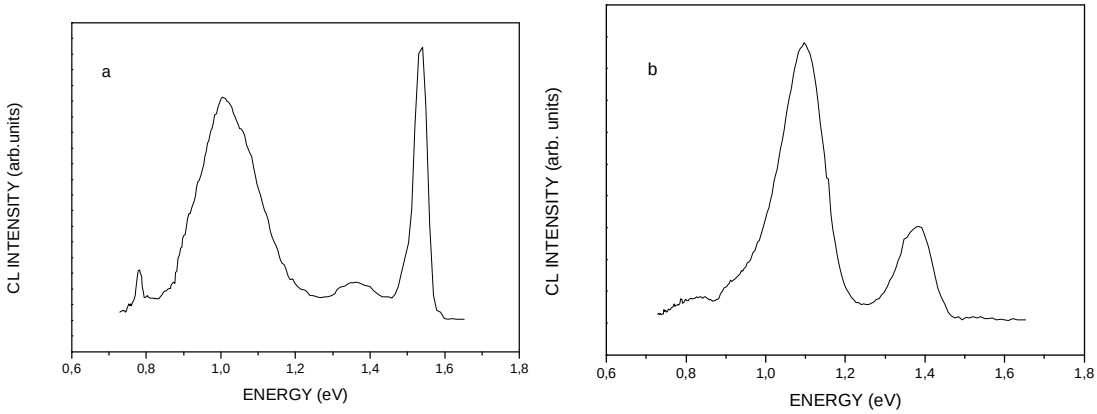

Fig. 8. CL spectra recorded at 80 K from a cross section of the as-grown CdTe wafer, with (a) focused and (b) defocused electron beam.

Fig. 8 shows typical CL spectra recorded from the cleaved surface of the as-grown sample. The spectra consist of three bands peaked at about 1.13, 1.4 and 1.54 eV. These bands have been attributed to the different complex defects in CdTe such as V_{Te} - V_{Cd} - impurity pairs and donor-acceptor pairs respectively [19,29,30]. After annealing in Ga melt the spectra were found to be modified and distinct in the different regions of the wafer volume. Fig. 9 shows the typical CL specta after 2 h annealing. The two lower energy bands disappear and the intensity of the 1.54 eV band is not homogeneous over the volume of the wafer (Fig. 9). The intensity decreased in the central part of the wafer cross section, also a decrease is observed near the surface in contact with the Ga melt. On the contrary the emission increased near the surface of the wafer exposed to vacuum.

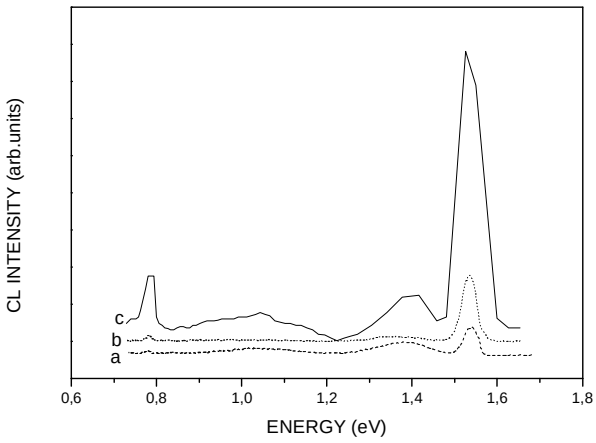

Fig. 9. CL spectra recorded at 80 K under focusing conditions of electron beam from the cross section of CdTe wafer annealed in the Ga melt at 600 ºC for 2 h: (a) in the region near the wafer surface in contact with the Ga melt; (b) in the central part of the cross section; (c) in the region near the wafer surface opposite to the Ga melt.

Fig. 10 shows the typical CL spectra of the long time annealed samples. These spectra demonstrate the lowest defect density in the central part of the wafer cross sections as after the short time annealing. In comparison with the spectra shown in Fig. 9 an increase of the 1.4 eV band can be observed all over the volume of the wafer. The 1.54 eV band shows an opposite behaviour to that reported above for the 2 h annealed sample, hence increasing intensity towards the center of the wafer cross section and the surface in contact with Ga melt, and decreasing in regions close to the surface exposed to vacuum. Fig. 11 shows an intensity profile of the 1.4 eV band obtained from the sample annealed for the longer time.

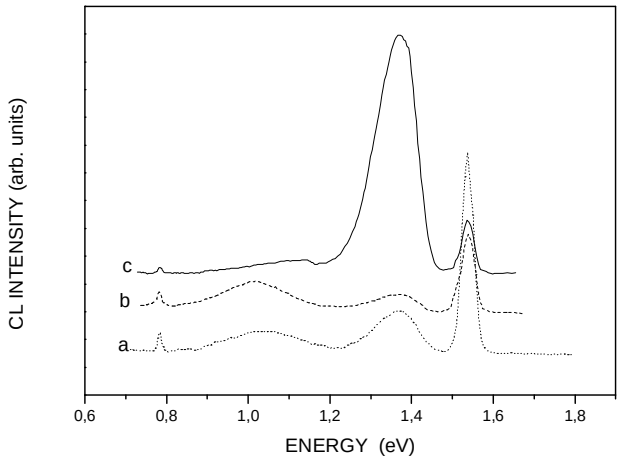

Fig. 10. CL spectra recorded at 80 K under focusing conditions of electron beam from the cross section of CdTe wafer annealed in the Ga melt at 600 ºC for 24 h: (a) in the region near the wafer surface in contact with the Ga melt; (b) in the central part of the cross section; (c) in the region near the wafer surface opposite to the Ga melt.

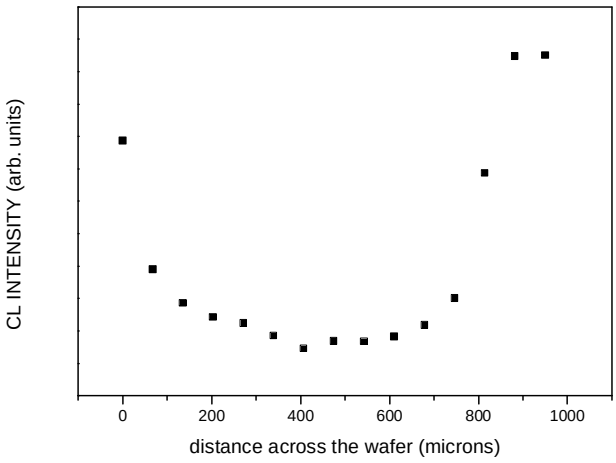

Fig. 11. Distribution of the 1.4 eV band intensity (80 K) across the cross section from the sample in 10b.

The behaviour of the 1.4 and 1.54 eV bands could be explained as a result of the in-diffusion of Ga atoms from the Ga melt, and the out-diffusion of Cd atoms from the surface exposed to vacuum. The Ga in-diffusion provides an increase in the concentrration of donors which are Ga atoms in Cd sites and the group I residual impurities in interstitials [29,30]. Simultaneously, it decreases the concentration of acceptors (Cd vacancies and the group I residual impurities in Cd sites) which causes the increase of intensities of the 1.4 and 1.54 eV bands near the wafer surfaces in contact with the Ga melt. Near the opposite surface, the out-

diffusion of Cd atoms is followed by an increase in the concentration of cadmium vacancies and decrease in the concentration of residual group I impurities in interstitial sites, hence the acceptor concentration becomes higher and the donor concentration lower, provoking an increase of the 1.4 eV band and a decrease of the 1.54 eV peak.

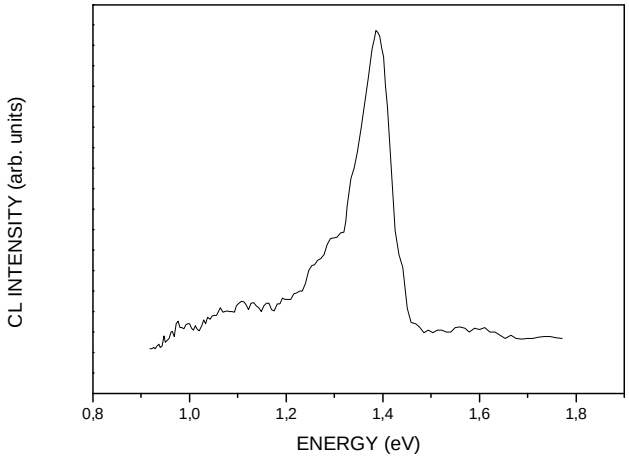

Fig. 12. CL spectrum of CdTe:Cl at 80 Kunder defocusing conditions of the electron beam.

After the annealing of as-grown samples in Cd vapour for 2 hours, the RS and CL spectra were similar to those obtained after 2 h Ga annealing. The long time annealing in Cd vapour causes the disappearance of Te precipitates in the central part of the wafer cross-section. The CL images showed a narrow precipitate free region 100-300 μm whose boundaries are not clearly defined unlike in the Ga annealing case. This difference could be due to the capability of Ga melt to dissolve the Te precipitates which migrate to the surface of the wafers during annealing. The effect of long time annealing in Cd vapour on the CL spectra were also similar to those obtained after Ga annealing shown in Fig. 10.

After annealing in vacuum the initial CL spectra do not change significantly, the distribution of Te precipitates is still random over the volume of the wafers, and only an increase in the concentration of Te precipitates is appreciated near both surfaces (Fig. 7d).

Since from the results described, most of the emissions seem to be related in some way to impurities, the influence of several dopants has been studied. In particular we have chosen Cl, V and Ge.

To study the influence of chlorine on the defect structure of CdTe not only as grown samples (type S1 and S3) were investigated, some samples were annealed under an argon flux at 600 °C for 5 hours. In some cases, cross-sectional observations of the wafers were performed on fresh cleaved surfaces to eliminate possible annealing induced surface effects [49]. Fig. 12 shows the spectrum of a Cl doped sample, obtained with defocused electron beam. With focused beam, emission was too low to record spectra with our detection system. In Fig. 12 only the 1.4 eV band is revealed with a shoulder in the 1.15 eV region. The effect of annealing on the CL spectra is also shown in Fig. 13. Annealing the undoped material causes the appearance of an intense band at 1.18 eV in addition to the 1.4 eV (Fig. 13a). In the Cl doped samples the effect of annealing is the enhancement of the 1.4 eV band while the emission in the range 1.05-1.20 eV is practically absent (Fig. 13b).

Panchromatic CL images of undoped samples show inhomogeneous distribution of luminescence intensity (Fig. 14a) with dark points in a bright background. Similar qualitative contrast is observed in monochromatic (λ=810 nm) images as well as in images recorded with emission above 1000 nm. Annealing causes enhancement of dark spots contrast. In Cl doped samples CL is inhomogeneous with a diffuse intensity distribution (Fig. 14b). The general appearance was not changed after annealing.

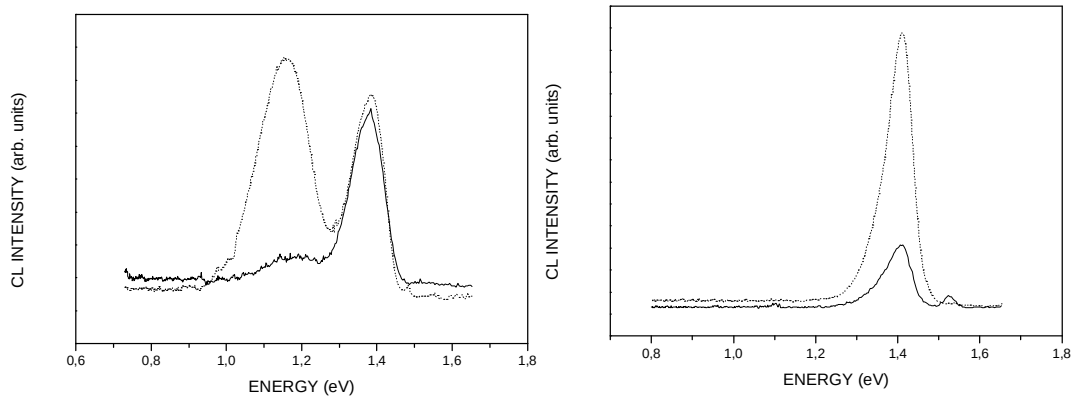

Fig. 13. a) Focused (—) and defocused (- - - -) CL spectra of undoped CdTe at 80 K after annealing at 600 ºC for 5 hrs in an inert atmosphere. b) Focused (——) and defocused (- - - -) CL spectra of CdTe:Cl at 80 K after annealing at 600 ºC for 5hrs in an inert atmosphere.

Undoped and Ge doped, as grown and annealed, samples (types S2 and S5) were studied, annealing was performed at 600 °C for 5 hrs under an Ar flux [50]. To avoid the annealing induced surface defects, the annealed wafers were polished again to remove about 50 μm from the surfaces. Fig. 15 shows a typical panchromatic CL image of the as-grown Ge doped samples (a:CdTe:Ge1; b:CdTe:Ge2). Bright sub-boundaries with a certain structure and bright spots inside the sub-grains are revealed. Typical CL spectrum of CdTe:Ge1 samples at 80 K is given in Fig. 16a. Under focusing or defocusing conditions of the electron beam no band edge peak or the generally referred 1.40 eV peak were clearly revealed. Under the focused electron beam condition, in all the doped samples, the total CL intensity was low and only a peak near 0.81 eV was revealed. By defocusing the electron beam, an intense band at about 0.91 eV and a very week band near 1.08 eV appeared along with the 0.81 eV band. It is observed in Fig. 16 that the 0.81 eV band appears more intense in the sample with higher Ge concentration.

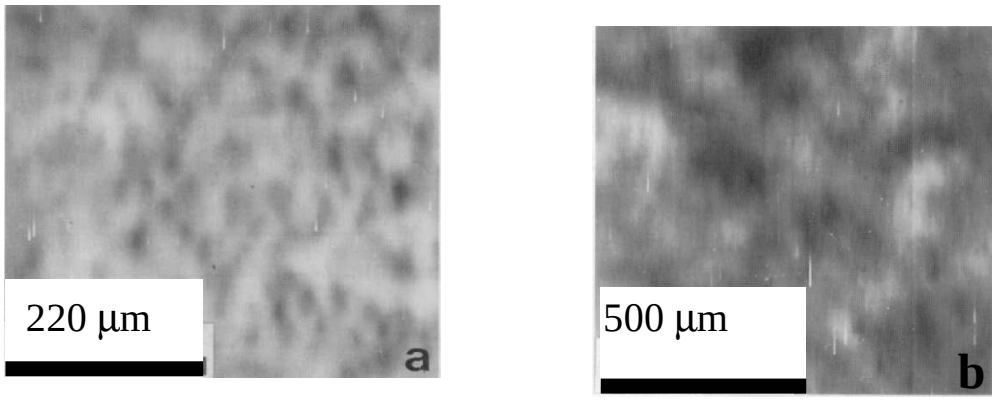

Fig. 14. Panchromatic CL images of a) undoped; b) CdTe:Cl; , recorded at 80 K.

Fig. 16c shows the CL spectra of the CdTe:Ge1 sample after annealing. No band edge peak or the 1.40 eV peak appeared under any of the electron beam conditions. However, both the 0.91 and 0.81 eV bands appeared under both electron beam conditions. There are at least four bands in the 0.72 eV - 1.10 eV energy range, often detected in CdTe crystals by other workers[51, 52] in their photoluminescence (PL)

studies. From the shape of the 0.91 eV band in our CL spectra, it appears that the band has at least three components. Though from the focused CL spectra the shorter wavelength component (or a separate peak) was resolved, we could not resolve the longer wavelength peaks with our existing detection system. In some cases, the 0.78 eV band was resolved (or a separate peak as in case of undoped samples) from the 0.81 eV band. As in the as-grown samples, the increase of the Ge concentration produces the increase of the 0.81 eV emission in the annealed samples (Fig. 16d). Fig. 17 shows the panchromatic CL image of an annealed CdTe:Ge1 sample at 80 K. By annealing, the sharper sub-boundaries become blurred and the contrast is drastically reduced. Monochromatic images recorded with the monochromatic slit at 0.90 eV or 0.80 eV exhibit the same general luminescence distribution as that shown in Fig. 15. After annealing, the general features in CL images of CdTe:Ge2 are very similar to the annealed CdTe:Ge1 samples. CL images of undoped samples show a well defined sub grain structure which is not modified by annealing [15].

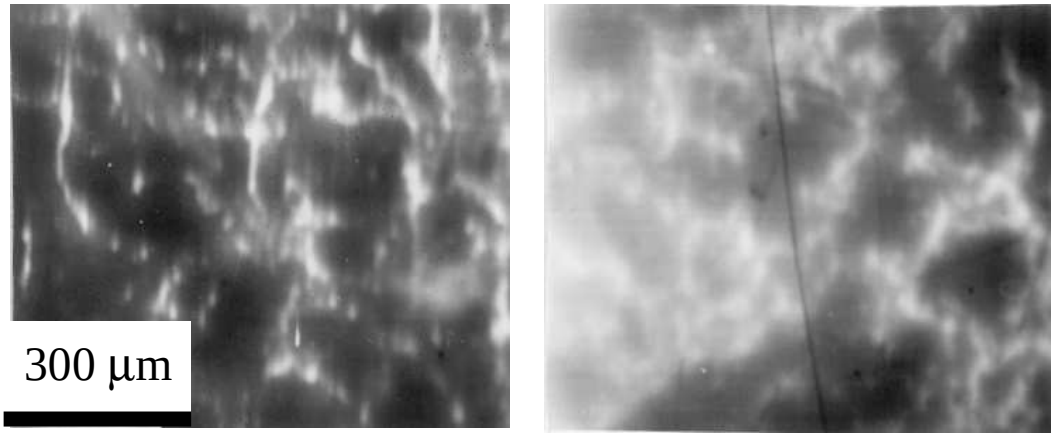

Fig. 15. Panchromatic CL image of as-grown CdTe:Ge1 (a) and CdTe:Ge2 (b).

As mentioned earlier, in undoped CdTe samples (type S2) the CL spectrum shows only the exciton band peaked at 1.54 eV when the electron beam is focused on the sample. By defocusing, the spectrum shows the 1.4 eV band. In contrast in CdTe:V samples (type S6) only the exciton band is observed even when the electron beam was defocused. After annealing in argon atmosphere at 600 ºC a band centred at 1.13 eV appears in both samples. Spectra of annealed samples are shown in Fig. 18.

Fig. 19 shows a typical CL image of the undoped sample with bright subboundaries and bright spots inside the subgrains. Images of V doped samples are similar but with a certain structure in the subboundaries (Fig. 19b). Annealing does not change the appearance of the CL image of undoped crystals but modifies markedly the CL of the doped samples. Instead of the well defined bright subboundaries of the unannealed samples dark regions appear in a brighter background. The contrast decreases in images recorded with a 1000 nm cut-on filter. Fig. 20 shows the CL images corresponding to V doped samples after annealing. The panchromatic CL images of CdTe:V annealed samples show a deep level luminescence with a distribution that cannot be easily related to a subgrain structure. The dark lobs in a brighter background indicate a redistribution of luminescent centres during annealing which could be related to V diffusion.

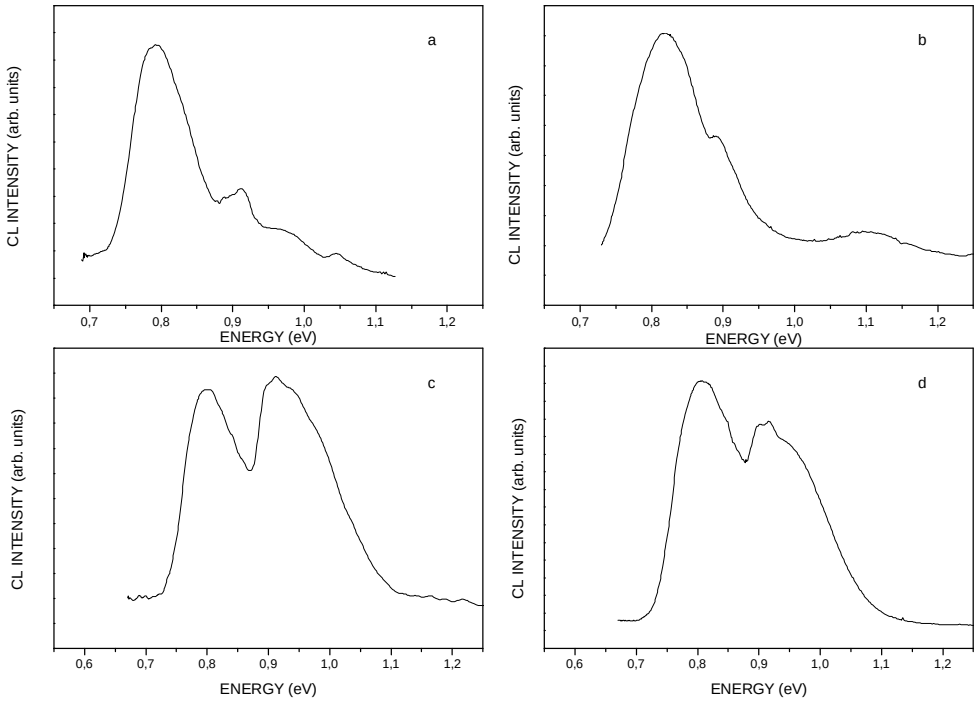

Fig. 16. CL spectra of as-grown a: CdTe:Ge1 and b: CdTe:Ge2; and annealed c: CdTe:Ge1 and d: CdTe:Ge2.

The 1.40 eV band in CdTe has a complex nature with a component, often determining the appearance of the band, due to A-centres (cadmium vacancy-donor pairs). This last fact explains the absence of 1.40 eV emission in some [19,49,50] doped samples. The undoped sample shows near band edge emission, the 1.4 band, a broad band centred at about 1.06 eV and a weak 0.781 eV emission, previously reported by other workers [53]. After annealing, the spectrum is dominated by a band at 1.18 eV probably due to the increase of one component of the broad 1.06 eV band. Emission at about 1.15 eV has been previously observed after annealing in inert atmosphere [19] and was thought to be the band attributed by Hofmann et al. [17] to tellurium vacancies. In our samples the band appears slightly shifted to higher energies. This is possibly due to a contribution of the 1.22 eV band revealed in some areas of the sample and also previously observed in doped and undoped CdTe [54]. Annealing in inert gas flow at 600 °C causes the formation of cadmium and tellurium vacancies and can therefore influence the 1.4 eV and 1.18 eV luminescence. The influence, however, depends on the impurities present in the sample. In undoped material the 1.18 eV band related to tellurium vacancies appears after annealing and the 1.40 eV band which has a component related to cadmium vacancies remains as an intense emission.

The different behaviour of undoped and V-doped samples could be related to the involvement of Cd vacancies -through A-centres- in the 1.40 eV emission. Since V is situated in substitutional Cd sites, a high concentration of V impurities can reduce the Cd-vacancy concentration and hence reduce the probability of A-centre formation and consequently the appearance of the 1.4eV band. Annealing causes the formation of cadmium and tellurium vacancies. This effect of annealing is more evident in V doped material. The unannealed samples had only band edge emission and the thermal treatment produces the two bands. These results agree with the suggestion of Cd and Te vacancies being involved respectively in the 1.40 eV and 1.13 eV luminescence observed in Ge doped samples. The Ge impurity situated in Cd sites reduces also the V_{Cd} concentration and consequently decreases the probability of A-centre formation. On the contrary, doping with atoms occupying Te sites in CdTe does not inhibit the appearance of the 1.40 eV band [55].

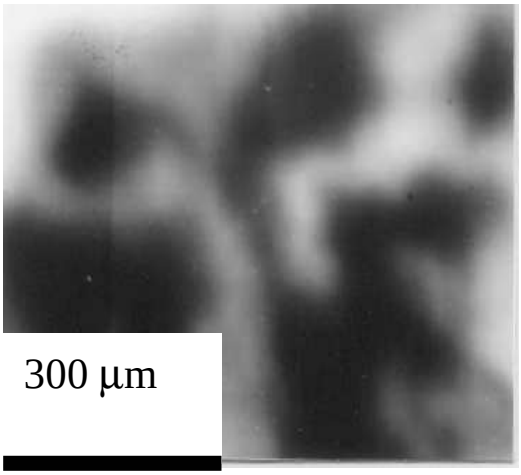

Fig. 17. Panchromatic CL image of annealed CdTe:Ge1.

In the low energy region of the spectra two bands centred respectively at about 0.91 and 0.81 eV are observed in doped and undoped samples. The bands are more intense in Ge doped samples suggesting the influence of Ge atoms. In particular the 0.81 eV band is always revealed as an intense emission in the spectra of doped samples while in undoped material is clearly revealed only under specific excitation condition (defocused electron beam). The influence of Ge on the 0.81 eV band is also apparent in its higher intensity in the CdTe:Ge crystals. The luminescence of CdTe in the 0.81 eV region has been found to consist of two overlapping sub-bands with maxima at 0.81 and 0.72 eV respectively [53,56]. Takebe et al. [57] characterised deep levels in CdTe by photo capacitance technique and deep level transient spectroscopy and concluded that a centre that can emit photons of 0.75 eV includes Cd vacancies or an impurity, as Si in Cd sites, whose solubility or stable site in the lattice depends on Cd vapour pressure. Emission in the 0.81 eV region in our undoped samples could be due, according with the results of ref. [55], to the Si residual impurity in CdTe. The observed enhancement of the 0.81 eV band in the Ge doped samples can be explained, by the fact that Ge plays a similar role as Si in the 0.81 eV emission. The band peaked at about 0.91 eV which is present in both kinds of samples but more readily observed in Ge doped crystals, can have a similar origin as the 0.81 eV emission. In a study of deep levels in CdTe by EPR techniques [57] a level at 0.95 eV below the conduction band edge was assigned to Ge dopant.

The results of annealing treatment support the possibility that Ge is involved in the emission at 0.91 eV and 0.81 eV. Annealing the undoped samples causes the increase of a band at 1.08 eV and the suppression of emission at lower energies. This 1.08 eV band has been previously reported in annealed undoped CdTe [19] and is attributed to the presence of Te vacancies. Annealing the Ge doped samples causes the increase of the 0.81 eV and 0.91 eV band as depicted in Fig. 18. During annealing, cadmium vacancies are generated and the probability of formation of complex centres involving Ge in Cd sites is enhanced. The diffuse appearance of luminescence in CL images of annealed samples indicates the redistribution and formation of luminescent centres during annealing related to vacancy generation and impurity diffusion processes. In chlorine doped samples the annealing induced vacancies can form complexes with the Cl donors, the chlorine A centre identified in [16], and cause the enhancement of the 1.4 eV emission. On the other hand substitutional Cl in Te sites reduce the numbers of Te vacancies causing a decrease of the 1.18 eV band. This emission, prominent in the undoped samples, has a residual character in the annealed CdTe:Cl. V situated in cadmium sites was used as impurity in CdTe and has an opposite behaviour to that of Cl impurities [19]. Due to the decrease of cadmium vacancies by V substitution, the 1.4 eV band was absent and appeared after annealing together with the 1.18 eV band.

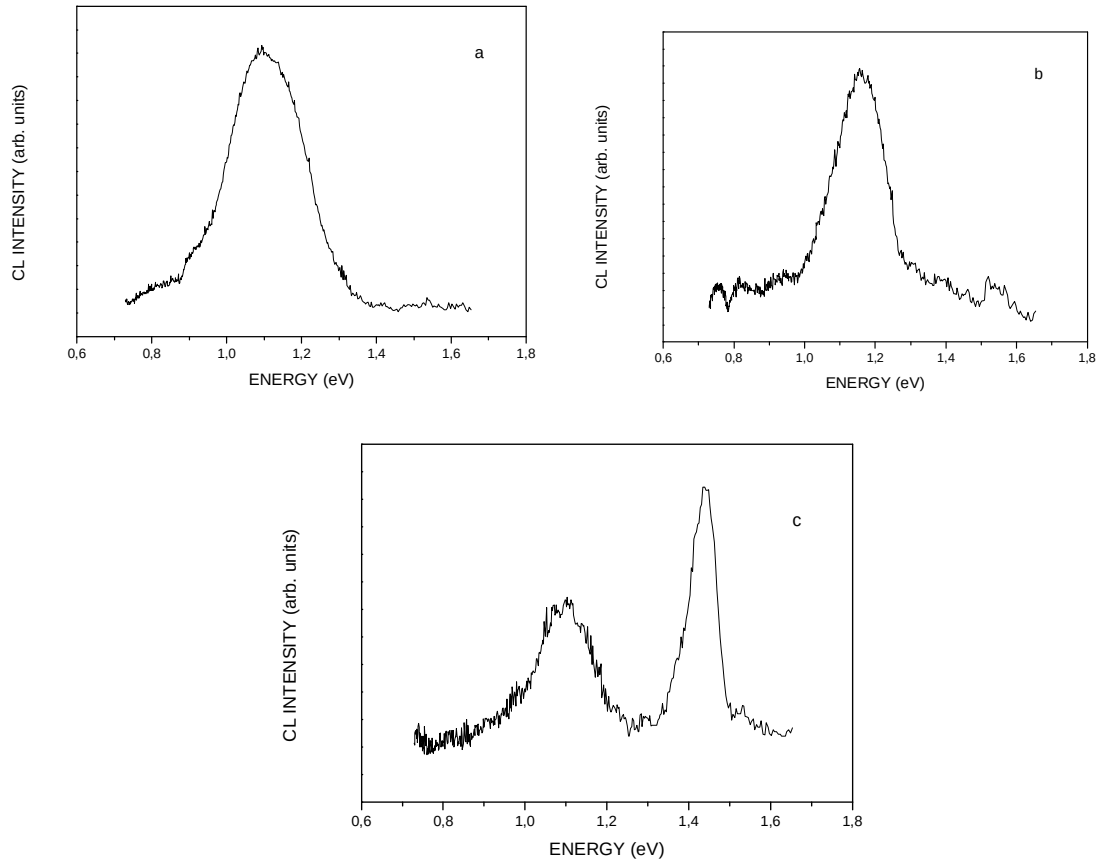

Fig. 18. CL spectra of annealed samples, recorded at 80 K.a)undoped CdTe; b)V doped sample, spectra recorded from the surface; c) V doped sample, spectra recorded from the cleaved edge.

Besides these doped samples, the CdTeZn system has been also studied. One of the advantages of this alloy is the possibility to tailor the band gap through variations in Zn concentration. The band gap can be varied from 1.45 eV (corresponding to CdTe) to 2.3 eV (corresponding to ZnTe) [58]. Also the lattice parameters can be matched to these of the CdHgTe alloys, thus inhibiting the formation of misfit dislocations during epitaxial growth. On the other hand this system allows us the study of the defects involved in the compensation mechanism, through the comparison with PICTS measurements [69,70]. The optical characterization of the samples (type S4) was carried out with CL experiments. Three bands peaked at 1.45 eV, 1.05 eV and 0.77 eV can be resolved.

To explain these results, one needs to take into account that Zn occupies Cd sites, thus decreasing the V_{Cd}^{+} concentration and increasing the material resistivity [59,60]. Moreover the band gap varies with Zn concentration according to the Varshni equation [61,62]. The valence band, associated to cadmium sublattice and related defects, does not shift much with increasing Zn concentration while conduction band, related to tellurium sublattice, rises markedly [17]. The comparison between the PICTS and the CL results obtained from these samples allows us to propose an attribution for the levels reported here. In the PICTS spectra a level at 0.16 eV is detected which is similar to that found for samples of different composition ($Cd_{0.9}Zn_{0.1}Te$) [63]. Some other techniques give also indication on a level at about 0.15 eV in CdTe which has been attributted to the center A [10,16,64-66]. Luminescence measurements on $Cd_{1-x}Zn_xTe$ reported in the literature attribute to this center an emission peaked at about 1.5 eV [16,61,67-70]. Such a band has also been found in our CL measurements on different kind of samples. Since the band gap of the $Cd_{0.8}Zn_{0.2}Te$ is 1.65 eV approximately, we can conclude that the PICTS level at 0.15 eV and the CL emission at 1.5 eV have the origin in the same defect, the centre A, also present in other doped samples. It has been proposed a complex structure for this centre (V_{Cd}^{-}-donor$_{Te}$) with acceptor character [16,66,67,71]. It has been

observed that the level associated to the centre A remains constant at E_v + 0.15 from CdTe (x = 0) [67,72] up to ZnTe (x = 1) while its associated luminescence energy increases as the band gap from CdTe (1.45 eV) to ZnTe (2.3 eV) [17]. The fact that the centre A follows the valence band behaviour confirms its attribution to the Cd sublattice [60].

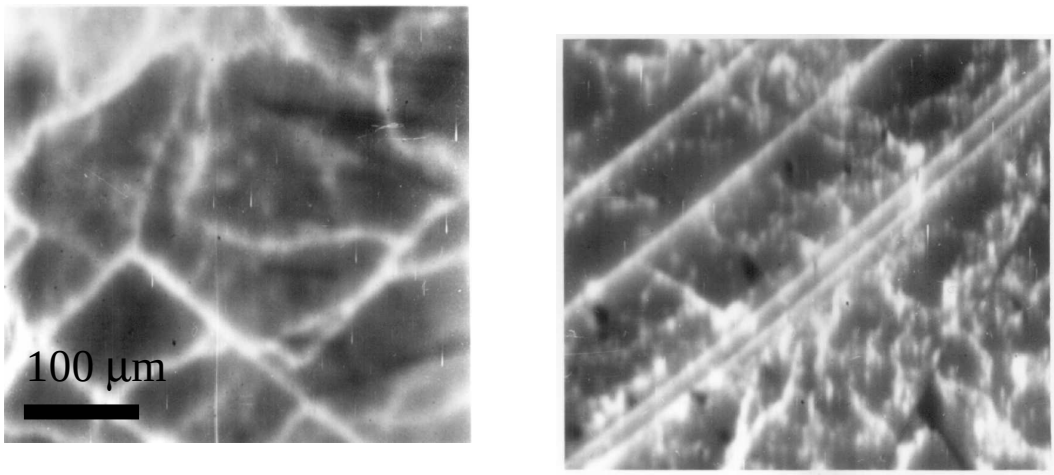

Fig. 19. Panchromatic CL image of (a) undoped CdTe and (b) CdTe:V, recorded at 80 K.

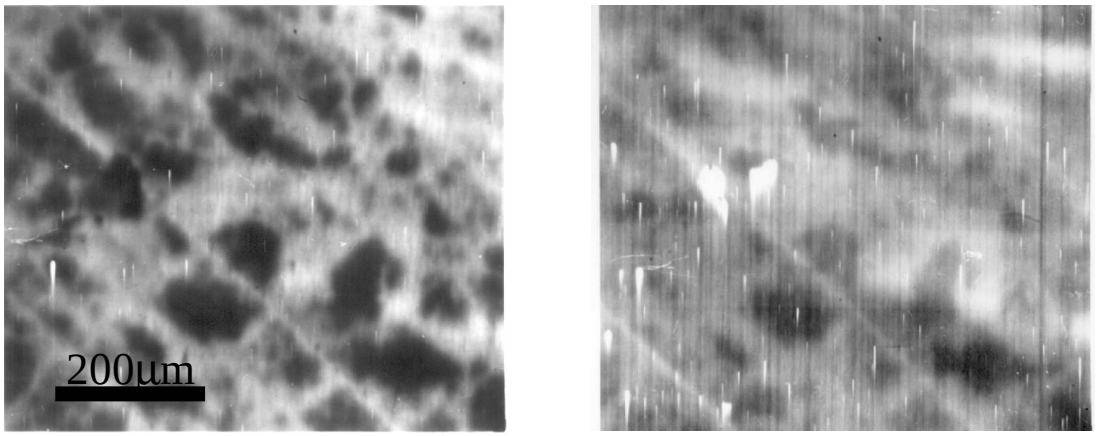

Fig. 20. CL images of annealed CdTe:V. (a) Panchromatic, (b) recorded with a 1000 nm cut on filter.

A PICTS level located at 0.25 eV [70] could be related to the level at 0.31 eV found in samples with 10% Zn concentration [63] or to the one at 0.27eV found in CdZnTe:In and also assigned to a Zn related defect [60]. This adscription to a Zn related defect is supported by the fact that no such level has been detected in undoped samples or in samples with dopants different than Zn [72]. In our CL measurements the band that could be associated to this level is one of the components of the 1.45 eV band, namely the one at 1.40 eV. However, we do not have sufficient information to identify the defect luminescence properties and, therefore, if its activation energy has to be measured from the valence or from the conduction band. Conductance measurements reported in the literature suggest that its activation energy is measured from the valence band and $E_a=E_v$+0.27 eV [60,73]. The PICTS level detected at 0.57 eV is attributted to any of the major traps found in CdTe [72], and appears to be present only in CdZnTe. The CL analysis does not straightforwardly suggest the existence of a band associated with this energy. However, it has been suggested that the defecct located at 0.55-0.65eV has an acceptor character and is related to a Zn vacancy [73]. The 0.78 eV peak reported from PICTS measurements [70] is the most prominent in our CL measurements on

$Cd_{0.8}Zn_{0.2}Te$ samples, and seems to be responsible for the control of transport processes [74-77]. It has been associated to a deep acceptor, V_{Cd}^{-}, which plays a crucial role in the compensation mechanism and in the pinning of the Fermi level [76, 78, 79]. More detailed investigations tend to attribute the level to the doubly ionized cadmium vacancy associated to an impurity [57,72] and have provided indication for its behaviour as a recombinaton center with $e_p \approx 5e_n$ [57]. This explains why it is detectable in DLTS in n- and p-type semiconducting samples [57,72,77]. Finally the CL emission peaked at about 1.05 eV which has been found in CdTe as well as in $Cd_{1-x}Zn_xTe$ samples and widely attributed to an intrinsic defect, likely V_{Te} [17,64,67,68], could be related to the level detected at 1.1eV in PICTS spectra. As this level is a donor, its activation energy has to be measured from the conduction band, $E_a = E_c$-1.1 eV [71].

The precedent considerations referred to possible adscriptions of the different defect levels encountered in these samples, but also some qualitative information can be gained through the investigation of spatial distribution of luminescence. CL images from the distribution of luminescence in undoped samples could be related to the existence of dislocations as non-radiative centers. According to the data of dislocation density provided by the suppliers most of the dark points can correspond to dislocations. The fact that the contrast does not change qualitatively in the different spectral regions shows that the non-radiative distributions are competing with radiative band edge and deep level transitions. Annealing enhances the dark regions contrast but no specific regions related to the 1.18 eV luminescence can be identified. This is partly due to the fact that the intense 1.18 eV emission is observed in defocused conditions. The diffuse (cloudy) appearance of CL images in Cl doped CdTe indicates a spatial distribution of recombination centers at microscopic scale but this distribution is not related to dislocations or other extended defects which are practically absent in this material.

In Ge-doped samples CL images show that centers emitting in the 0.70 - 0.91 eV range which are responsible for the luminescence are preferentially distributed in the sub-boundaries. The grainy structure of sub-boundaries in the CL images has been observed in other doped CdTe crystals [19] and indicates an inhomogeneous distribution of luminescence centers along the sub-boundaries. However, on increasing the Ge atom concentration, these centers become more concentrated at the sub-boundaries. On the other hand CL images show that the defect emission has an inhomogeneous distribution in the sample and is mainly localized, similar to exciton emission, at subgrain boundaries. Surface defect emission generated by polishing treatment would rather show a more uniform distribution. Part of the defect luminescence seems to be related to defects decorating subboundaries and dislocations.

Finally it is worth noting that the 1.4eV band is influenced by surface treatment of the sample and part of the emission can be directly related to surface defects [12]. However Bubulac et al. [13] concluded, contrary to previous results, that a low intensity of the 1.4 eV band relative to the exciton peak is not an indication of good crystal quality. Some of the present results support this conclusion and indicate that the 1.4 eV band is not only related to surface defects. In our spectra obtained with focused electron beam only the exciton luminescence is observed which indicates that defects responsible for the 1.4 eV band are present in low concentrations. In the undoped crystals the band appears by defocusing as a consequence of a higher sample volume being excited by the electron beam. The V-doped samples do not reveal the 1.4 eV band in any experimental conditions. Both samples show similar CL images with dislocations and subboundaries. The lack of the 1.4 eV emission in the V-doped sample could be an effect of the presence of V as mentioned earlier. This impurity could introduce recombination paths competing with the 1.4 eV band. The fact that intensity of the 1.4 eV band shows an U-shaped profile supports the possibility that bulk defects are involved in the emission. This distribution has been often related to thermal stresses and other effects appearing in the ingot during crystal growth.

4. Conclusions

Impurities in CdTe influence in several ways the luminescence emissions. While V impurities inhibit the appearance of 1.4 eV band, Cl doping enhances this emission. Like V atoms, Ge plays a similar role compensating Cd vacancies and reduces the possibility of A-center formation in CdTe crystals. Appearance of 0.81 eV emission in CdTe crystals can be influenced very much by Ge doping. Annealing behaviour depends also on dopants. In undoped material the spectrum is dominated by the Te vacancy related emission

(1.13 eV), however in V doped samples, annealing in inert atmosphere causes the appearance of both 1.4 and 1.13 eV emission. The behaviour under annealing treatment of Ge doped samples, indicates that one way to control the appearance and intensity of the 1.4 eV band is to dope with substitutional impurities influencing the formation of the A- centers involved in the emissions. In undoped CdTe, either annealed or unannealed, the contribution of 0.91 and 0.81 eV bands is minor to the total luminescence.

Indentation in CdTe crystals causes quenching of total CL intensity. Besides non radiative recombination centers, radiative centers related to Cd and Te vacancies are generated during deformation. Annealing induced changes in the CL images of indentation are mainly due to decoration processes by impurities.

Acknowledgements

The experiments presented in this work have performed during a long time and several researchers have collaborated with their effort. In particular part of the measurements have been done by Dr. U. Pal and Dr. Díaz-Guerra, the fruitful discussions with them and very specially with Prof. J. Piqueras are acknowledged.

The research have been performed in the frame of different projects of the Spanish agencies for science and technology PB 90-1017, PB-93-1256, PB96-0639, MAT2000-2119.

CdTe samples were kindly supplied by Japan Energy Corporation.

Reference

[1] M. Ohmori, Y. Iwase, R. Ohno, Mat. Sci. and Eng. **B16**, 283 (1993).
[2] H. Tsutsui, T. Ohtsuchi, K. Ohmori, S. Baba, Jpn. J. Appl. Phys. **32**, 228 (1993).
[3] J. R. Pugh, D. Mao, J. G. Zhang, M. J. Heben, A. J. Nelson, A. J. Frank, J. Appl. Phys. **74**, 2619 (1993).
[4] J. Britt, C. Ferekides, Appl. Phys. Lett. **62**, 2851 (1993).
[5] N. V. Sochinskii, Proc. of the Workshop on Advanced Infrared Technology and Application, Florence, April 1992, edited by G. M. Carlomagno and C.Corsi (Florence 1993) p. 29.
[6] N. V. Sochinskii, M. D. Serrano, S. Bernardi, E. Diéguez, Proc. of the Workshop on Advanced Infrared Technology and Application, Capri, September 1993, edited by L. Ronchi Abozzo, G. M. Carlomagno, C. Corsi (Florence 1994) p. 43.
[7] R. B. Bylsma, P. M. Bridenbaugh, D. H. Olson, A. M. Glass, Appl. Phys. Lett. **51**, 889 (1987).
[8] A. Partovi, J. Millerd, E. M. Garmine, M. Ziari, W. H. Steier, S. B. Trivdi, M. B. Klein, Appl. Phys. Lett. **57**, 846 (1990).
[9] N. V. Sochinskii, V. N. Babentsov, N. I. Tarbaev, M. D. Serrano, E. Diéguez, Mat. Res. Bull., **28**, 1061 (1993) and references therein.
[10] C. Eiche, D. Maier, D. Sinerius, J. Weese, K. W. Benz, J. Honerkamp, J. Appl. Phys. **74**, 6667 (1993).
[11] V. P. Zayachkivskii, A. V. Savitskii, E. S. Nikonyuk, M. S. Kitsa, V. V. Matlak, Sov. Phys. Semicond. **8**, 675 (1974).
[12] T. H. Myers, J. F. Schetzina, S. T. Edwards, A. F. Schrein, J. Appl. Phys. **54**, 4232 (1983).
[13] L. O. Bubulac, J. Bajaj, W. E. Termant, P. R. Newman, D. S. Lo, J. Cryst. Growth, **86**, 536 (1988).
[14] H. L. Cotal, A. C. Lewandowski, B. G. Markey, S. W. S. Mc Keever, E. Cantrell, J. Aldridge, J. Appl. Phys. **67**, 975 (1990).
[15] U. Pal, P. Fernández, J. Piqueras, M. D. Serrano, E. Diéguez, Inst. Phys. Conf. Ser. nº135, 177 (1994).
[16] D. M. Hofmann, P. Omling, H. G. Grimmeiss, B. K. Meyer, K. W. Benz, D. Sinerius, Phys. Rev. **B45**, 6247 (1992).
[17] D. M. Hofmann, W. Stadler, K. Oettinger, B. K. Meyer, P. Omling, M. Salk, K. W. Benz, E. Wiegel, G. Müller-Vogt, Mat. Sci. and Eng. **B16**, 128 (1993).

[18] F. J. Bryant, E. Webster, phys. stat. sol. (b) **49**, 499 (1972).
[19] U. Pal, J. Piqueras, P. Fernández, M. D. Serrano, E. Diéguez , J. Appl. Phys **76**, 3720 (1994).
[20] P. A. Slodowy, J. M. Baranowski, phys. stat. sol. (b) **49**, 499 (1972).
[21] N. I. Tarbaev, G. A. Shepelskii, J. Schreiber, Soviet Phys. Solid State **31**, 1348 (1989).
[22] V. N. Babentsov, S. I. Gorban, E. A. Salkov, N. I. Tarbaev, Soviet Phys. Semicond. **21**, 1043 (1987).
[23] S. Sen, W. H. Konkel, S. J. Tighe, L. G. Bland, S. R. Sharma, R. E. Taylor, J. Cryst. Growth **86**, 111 (1988).
[24] H. G. Brion, C. Mewes, I. Hahn, U. Schaufele, J. Cryst. Growth **134**, 281(1993).
[25] H. N. Jayatirtha, D. O. Henderson, A. Burger, M. P. Volz, Appl. Phys. Lett. **62**, 573 (1993).
[26] H. R. Vydyanath, J. A. Ellsworth, J. B. Parkinson, J. J. Kennedy, B. Dean, C. J. Johnson, G. T. Neugebauer, J. Sepich, P. K. Liao, J. Electron. Mater. **22**, 1073 (1993).
[27] K. Peters, A. Wenzely P. Rudolph, Cryst. Res. and Tech. **25**, 1107 (1990) and references therein.
[28] E. D. Jones, J. Malzbender, J. B. Mullin, N. Shaw, J. Phys: Cond. Matter. **6**, 7499 (1994).
[29] N. V. Sochinskii, M. D. Serrano, V. N. Babentsov, N. I. Tarbaev, J. Garrido, E. Diéguez, Semicond. Sci. Techn. **9**, 1713 (1994).
[30] N. V. Sochinskii, V. N. Babentsov, N. I. Tarbaev, M. D. Serrano, E. Diéguez, Mater. Res. Bull. **28**, 1061 (1993).
[31] M. Koralewskii, N. V. Sochinskii, M. D. Serrano, E. Diéguez, J. Garrido, G. Lifante, B. Noheda, J. A. Gonzalo, Appl. Phys. Comm. **13**, 69 (1994).
[32] N. V. Sochinskii, V. N. Babentsov, S. V. Kletskii, M. D. Serrano, E. Diéguez, phys. stat. sol. (a) **40**, 445 (1993).
[33] J. C. Tranchart, P. Bach, J. Cryst. Growth **32**, 8 (1976).
[34] K. Mochizuki, T. Yoshida, K. Igaki, T. Shoji, Y. Hiratate, J. Cryst. Growth **73**, 123 (1985).
[35] S. H. Shin, J. Bajaj, L. A. Moudy, D. T. Cheung, Appl. Phys. Lett. **43**, 68 (1983).
[36] W. J. Kim, M. J. Park, S. D. U. Kim, T. J. Lee, J. M. Kim, W. J .Song, S. H. Suh, J. Cryst. Growth **104**, 677 (1990).
[37] F. Domínguez-Adame, J. Piqueras, P. Fernández, Appl. Phys. Lett. **58**, 257 (1991).
[38] Point and Extended Defects in semiconductors, edited by G. Benedek, A. Cavallini, W. Schröter (Plenum, New York, 1989).
[39] D. B. Holt, SEM Microcharacterization of Semiconductors edited by D.B. Holt, D. C. Joy (Academic Press 1989), p. 241.
[40] H. C. Casey, J. S. Jayson, J. Appl. Phys. **42**, 2774 (1971).
[41] A. Rivière, B. Sieber, J. P. Rivière, Microscopy Microanalysis Microstructures **2**, 257 (1991).
[42] A. Urbieta, P. Fernández, J. Piqueras, Ch. Hardalov, T. Sekiguchi, J. Phys. **D34**, 2945 (2001).
[43] O. Brümmer, J. Schreiber, Kristall und Technik **7**, 683 (1972).
[44] P. Fernández, J. Piqueras, A. Urbieta, T. Rebane, Y. Shreter, Semicon. Sci. and Tech. **14**(1), 430 (1999).
[45] A.Urbieta, P. Fernández, J. Piqueras, V. Muñoz, Mat. Sci. and Eng. **B78**, 105 (2000).
[46] J. A. García, A. Remón, P. Fernández, J. Piqueras, V. Muñoz, Semicond. Sci. and Tech. **16**, 289 (2001).
[47] R. M. Amirtharaj, F. H. Pollack, Appl. Phys. Lett. **45**, 789 (1984).
[48] N. V. Sohinskii, E. Diéguez, U. Pal, P. Fernández, J. Piqueras, F. Agulló-Rueda, Semicond. Sci. and Techn. **11**, 1354 (1996).
[49] U. Pal, P. Fernández, J. Piqueras, Mat. Letters **23**, 227 (1995).
[50] U. Pal, P. Fernández, J. Piqueras, N. V. Sochinnskii, E. Diéguez, J. Appl. Phys. **78**(3) 1992 (1995).
[51] S. Sen, W. H. Konkel, S. J. Tighe, L. G. Bland, S. R. Sharma, R. E. Taylor, J. Cryst. Growth **86**, 111 (1988).
[52] J. C. Tranchart, P. Bach, J. Cryst. Growth **32**, 8 (1976).
[53] J. Krustok, A. Loo, T. Piibe, J. Phys. Chem. Solids **52**, 1037 (1991).
[54] E. Weigel, G. Müller-Vogt, B. Steinbach, W. Wendl, W. Stadler, D. M. Hofmann B. K. Meyer, Mat. Sci., Eng. **B16**, 17 (1993).

[55] U. Pal, P. Fernández, J. Piqueras, unpublished results.
[56] Yu. I. Krustak, T. E. Piibe, A. E. Lyo, Sov. Phys. Semicond. **25**, 759 (1991).
[57] T. Takebe, J. Saraie, H. Matsunami, J. Appl. Phys. **53**, 457 (1992).
[58] C. Norris, K. Zanio, J. Appl. Phys. **53**, 6347 (1982).
[59] S. Fuyuki, N. Hyakutake, S. Hayakawa, Jpn. J. App. Phys. **17**, 851 (1978).
[60] K. Suzuki, K. Inagaki, N. Kimura, I. Tsubono, T. Sawada, K. Imai, S. Seto, phys. stat. sol. (a) **147**, 203 (1995).
[61] Y. P. Varshni, Physica **34**, 149 (1967).
[62] E. López-Cruz, J. González-Hernández, D. Dallred, W. P. Allred, J. Vac. Sci. Technol. **A8**, 1934 (1990).
[63] M. Fiederle, D. Ebling, C. Eiche, D. M. Hofmann, M. Salk, W. Stadler, K. W. Benz, B. K. Meyer, J. Cryst. Growth **138**, 524 (1994).
[64] J. P. Zielinger, M. Tapiero, Z. Guellil, G. Roosen, P. Delaye, J. C. Launay, W. Mazoyer, Mat. Sci. Eng. **B16**, 273 (1993).
[65] M. Samimi, B. Biglari, M. Hage-Ali, J. M. Koebel, P. Siffert, phys. stat. sol. (a) **100**, 251 (1987).
[66] M. Hage-Ali, P. Siffert, Nucl. Instr. and Meth. **A322**, 313 (1992).
[67] W. Stadler, D. M. Hoffman, H. C. Alt, T. Muschik, B. K. Meyer, E. Weigel, G. Müller-Vogt, M. Salk, E. Rupp, K. W. Benz, Phys. Rev. **B51**, 10619 (1995).
[68] C. Barnett Davis, D. D. Allred, A. Reyes-Mena, J. González-Hernández, O. Gonzáles, B. C. Hess, W. P. Allred, Phys. Rev. **B47**, 13363 (1993).
[69] A. Castaldini, A. Cavallinin, B. Fraboni, L. Polenta, P. Fernández, J. Piqueras, Mat. Sci. and Eng. **B42**, 302 (1996).
[70] A. Castaldini, A. Cavallinin, B. Fraboni, L. Polenta, P. Fernández, J. Piqueras, Pys. Rev. **B56**(23), 14897 (1997).
[71] J. W. Allen, Semicond. Sci. Technol. **10**, 1049 (1995).
[72] Private communication.
[73] T. L. Larsen, C. F. Vaarotto, D. A. Stevenson, J. Appl. Phys. **43,** 172 (1972).
[74] E. Rzepka,Y. Marfaing, M. Cuniot, R. Triboulet, Mat. Sci. and Eng. **B16**, 262 (193).
[75] H. X. Han, B. J. Feldman, M. L. Wroge, D. J. Leopold, J. M. Ballingall, J. Appl. Phys. **61**, 2670 (1987).
[76] P. Moravec, M. Hage-Ali, L. Chibani, P. Siffert, Mat. Sci. and Eng. **B16**, 223 (193).
[77] C. Ye, J. H. Chen, J. Appl. Phys. **67**, 2475 (1990).
[78] P. Höschl, P. Moravec, J. Franc, E. Belas, R. Grill, Nucl. Inst. and Meth. **A322**, 371 (1992).
[79] N. V. Agrinskaya, E. N. Arkadeva, Nucl. Inst. and Meth. **A283**, 260 (1992).